Electronic Supplementary Material (ESI) for RSC Advances.

Supporting Information

Cucurbit[7]uril-tetraphenylethene Host-guest System Induced Emission Activity

Rong Jiang, Shuang Wang, and Jinping Li

Caption of Content

Scheme S1. Synthesis of the guest TATPE.

Figure S1. ^{1}H NMR spectrum of **2** recorded in D_2O at 25°C.

Figure S2. ^{1}H NMR and ^{13}C NMR spectra of TATPE recorded in D_2O at 25°C.

Figure S3. Partial NOESY NMR spectrum of the complex Q[7]-TATPE recorded in D_2O at 25°C.

Figure S4. The MALDI-TOF mass spectrum of Q[7]-TATPE.

Figure S5. Job's plot of ΔF in fluorescence intensity of guest TATPE *versus* the molar ratio of $N_{TATPE}/(N_{TATPE} + N_{Q[7]})$ in water.

Figure S6. The TEM image of Q[7]-TATPE (A) and the enlarged TEM image of A (B).

Figure S7. ^{1}H NMR spectra of TATPE (A), the complex Q[7]-TATPE (B), adding 15.0 equiv. Ada to B (C), the complex Q[7]-Ada (D), and Ada (E) recorded in D_2O at 25°C.

Figure S8. Curves of fluorescence intensity *versus* the molar ratio of $N_{Ada}/N_{Q[7]}$ measured at 464 nm and 396 nm in water.

Table S1. Complex stability constant (K_a), enthalpy ($\Delta H°$), and entropy changes ($T\Delta S°$) for Q[7]-TATPE.

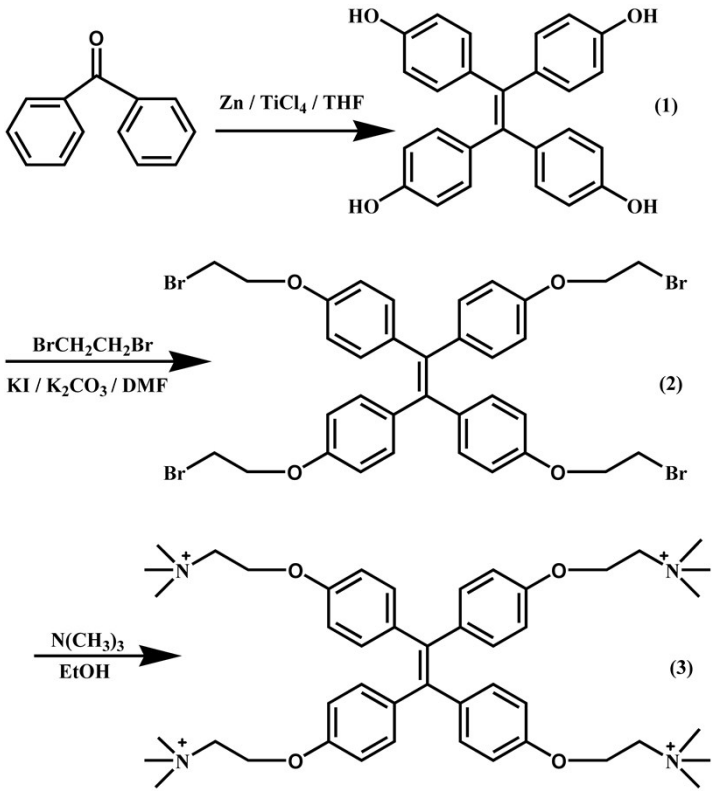

Scheme S1. Synthesis of the guest TATPE.

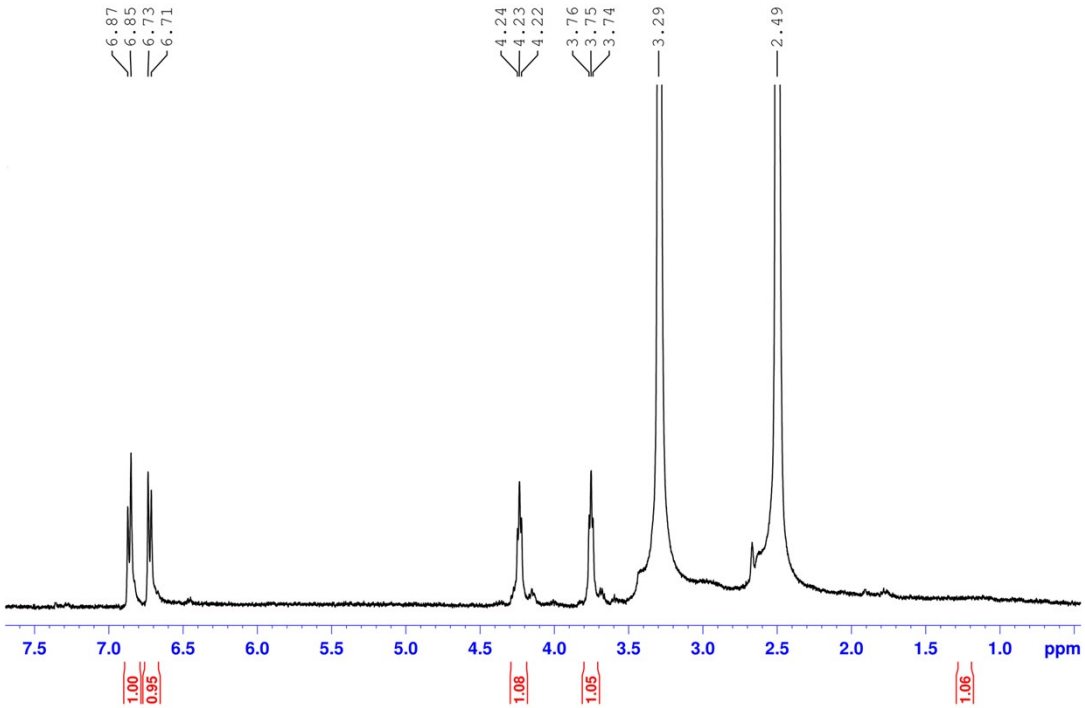

Figure S1. ^{1}H NMR spectrum of **2** recorded in D_2O at 25°C.

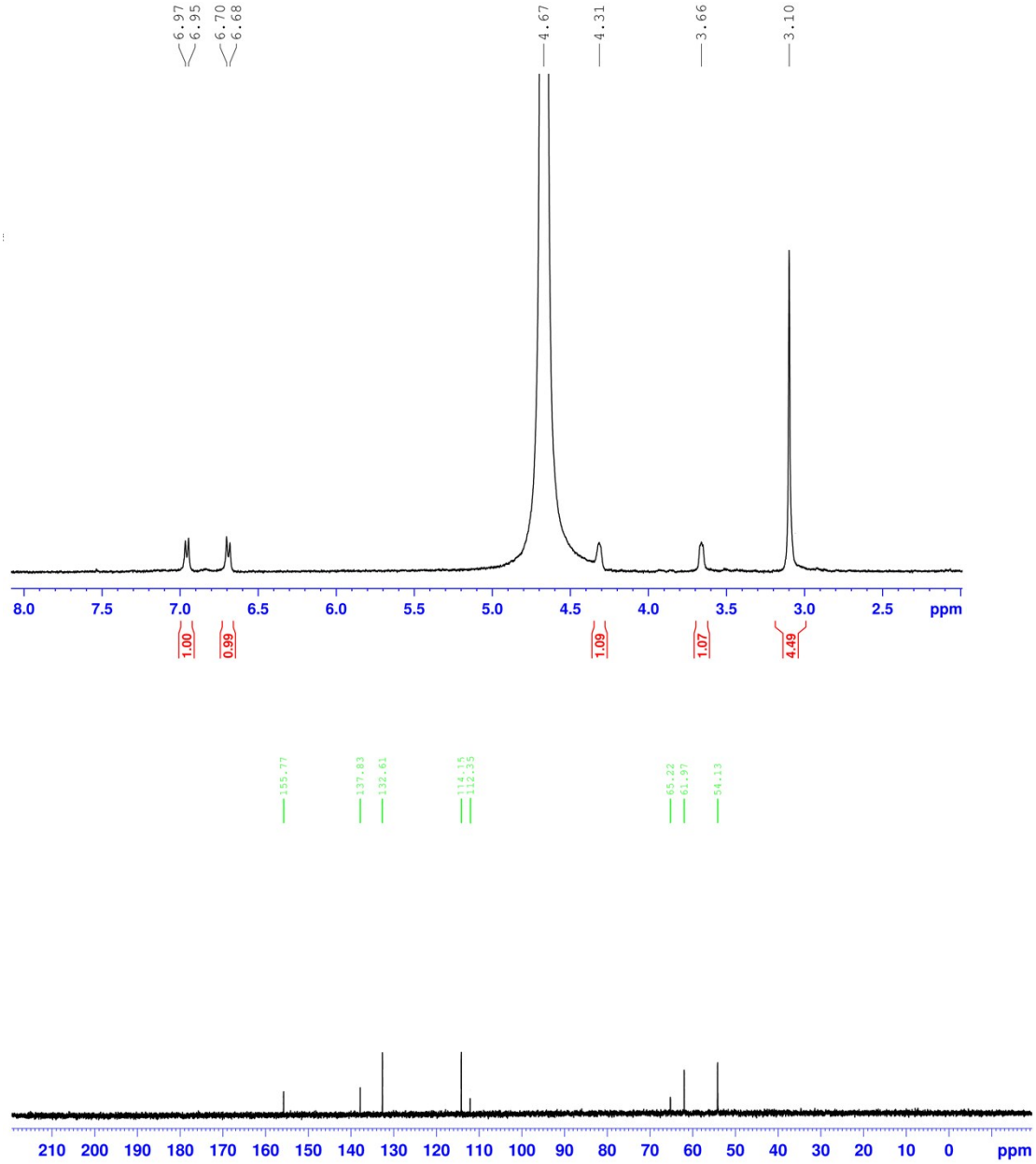

Figure S2. ^{1}H NMR and ^{13}C NMR spectra of TATPE recorded in D_2O at 25°C.

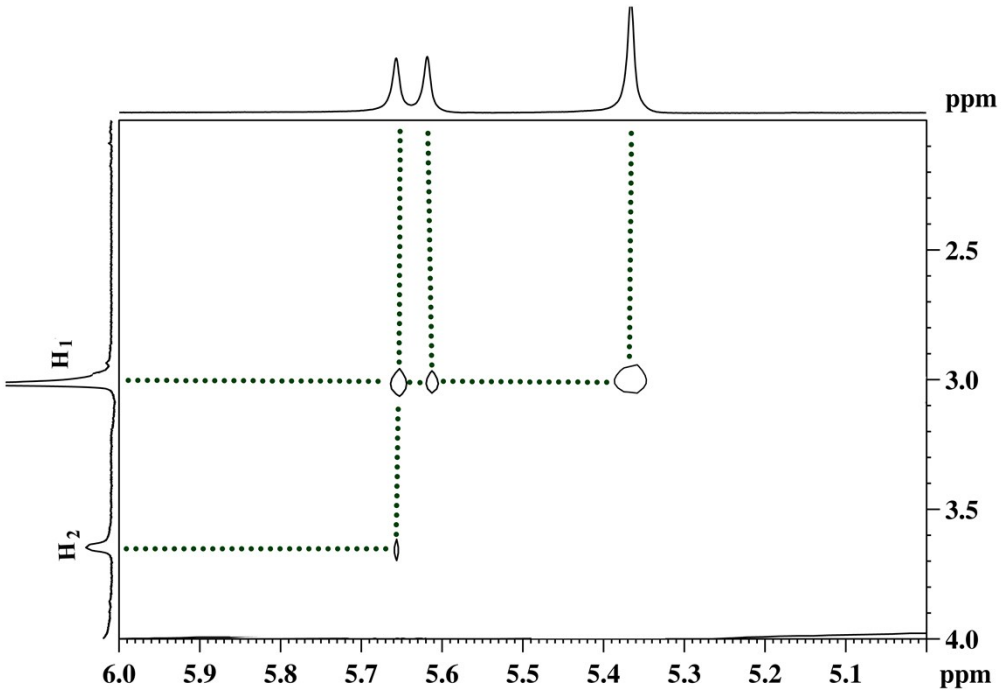

Figure S3. Partial NOESY NMR spectrum of the complex Q[7]-TATPE recorded in D_2O at 25°C.

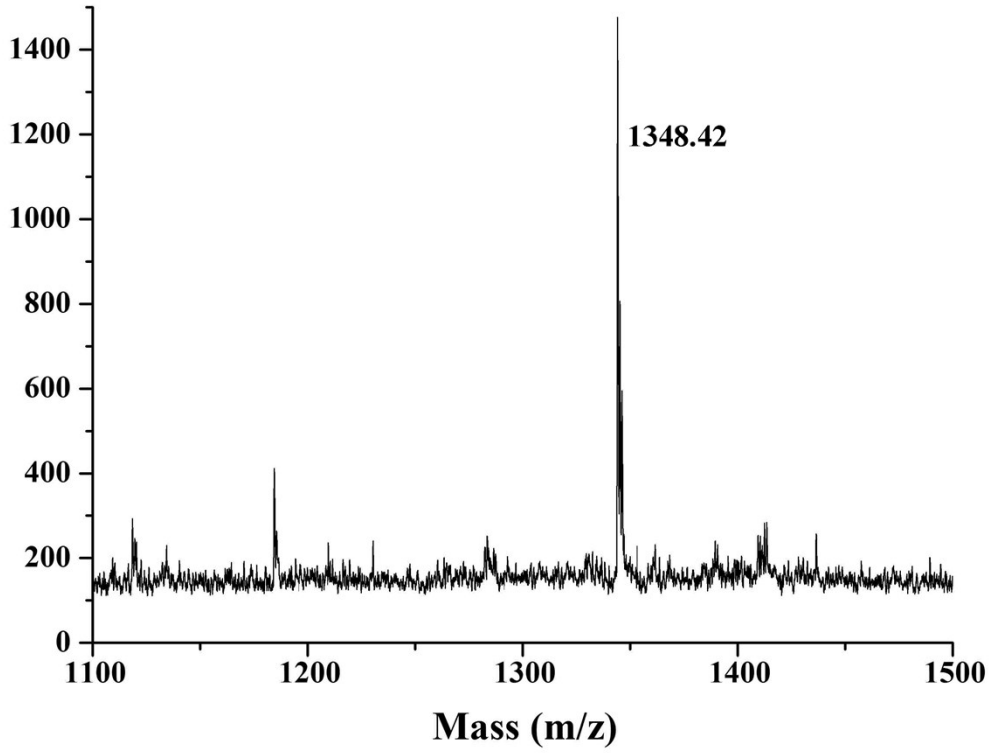

Figure S4. The MALDI-TOF mass spectrum of Q[7]-TATPE. It is worth noting that the MALDI-TOF mass spectroscopic results, Figure S4, provide direct support for the formation of the host-guest inclusion complex Q[7]-TATPE. The strongest peak found at *m*/*z* 1348.42 corresponds to $\{4Q[7]\text{-}TATPE{-}4Br^{-}\}^{4+}$.

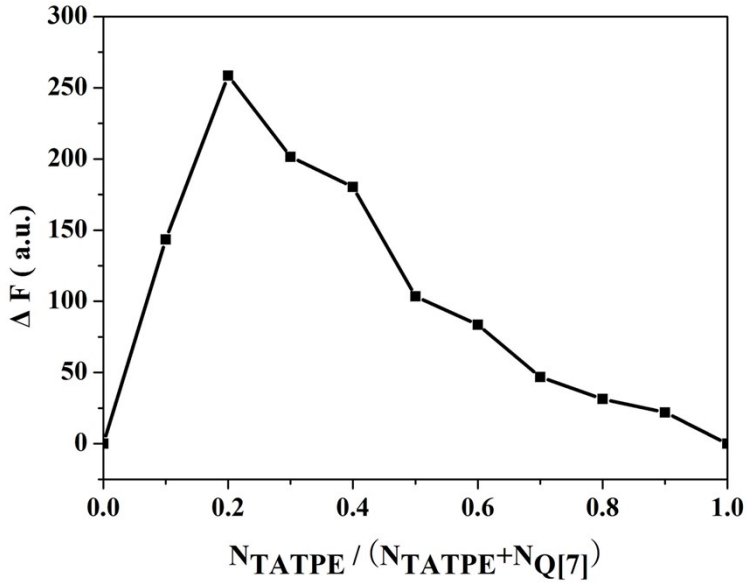

Figure S5. Job's plot of ΔF in fluorescence intensity of guest TATPE *versus* the molar ratio of $N_{TATPE}/(N_{TATPE} + N_{Q[7]})$ in water.

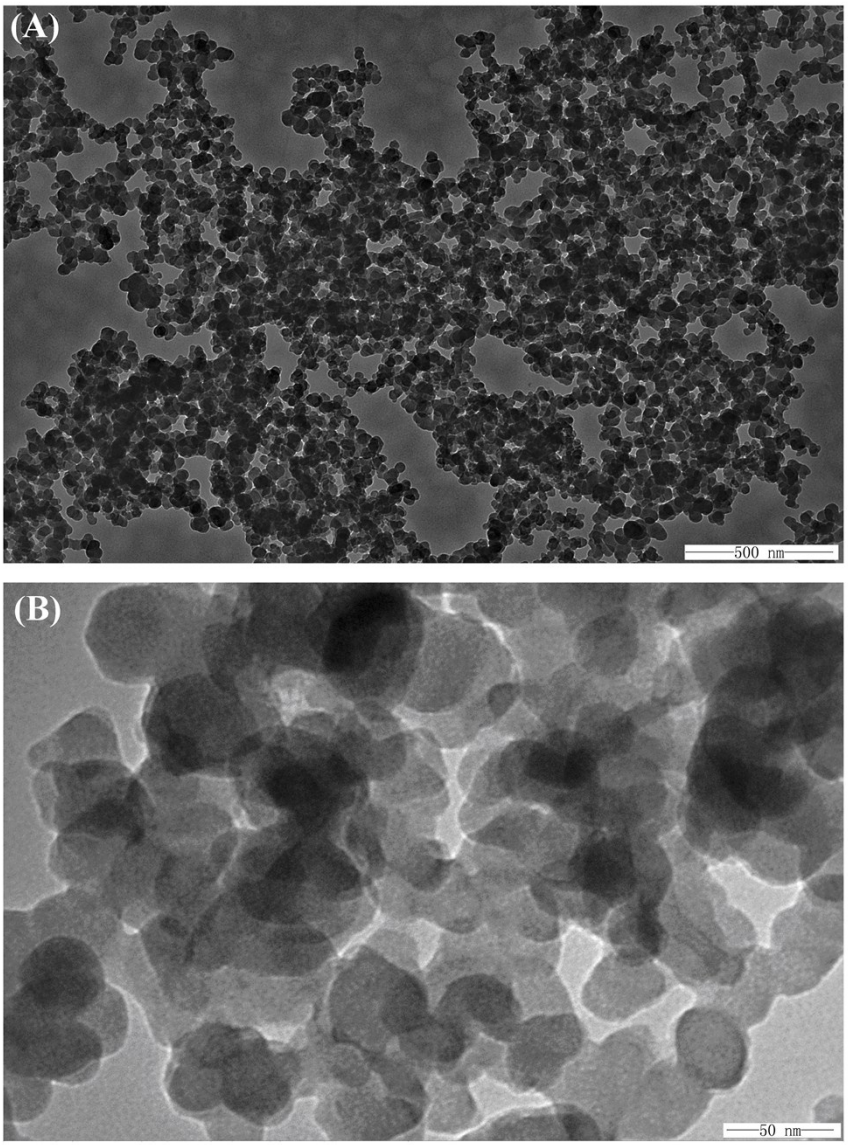

Figure S6. The TEM image of Q[7]-TATPE (A) and the enlarged TEM image of A (B).

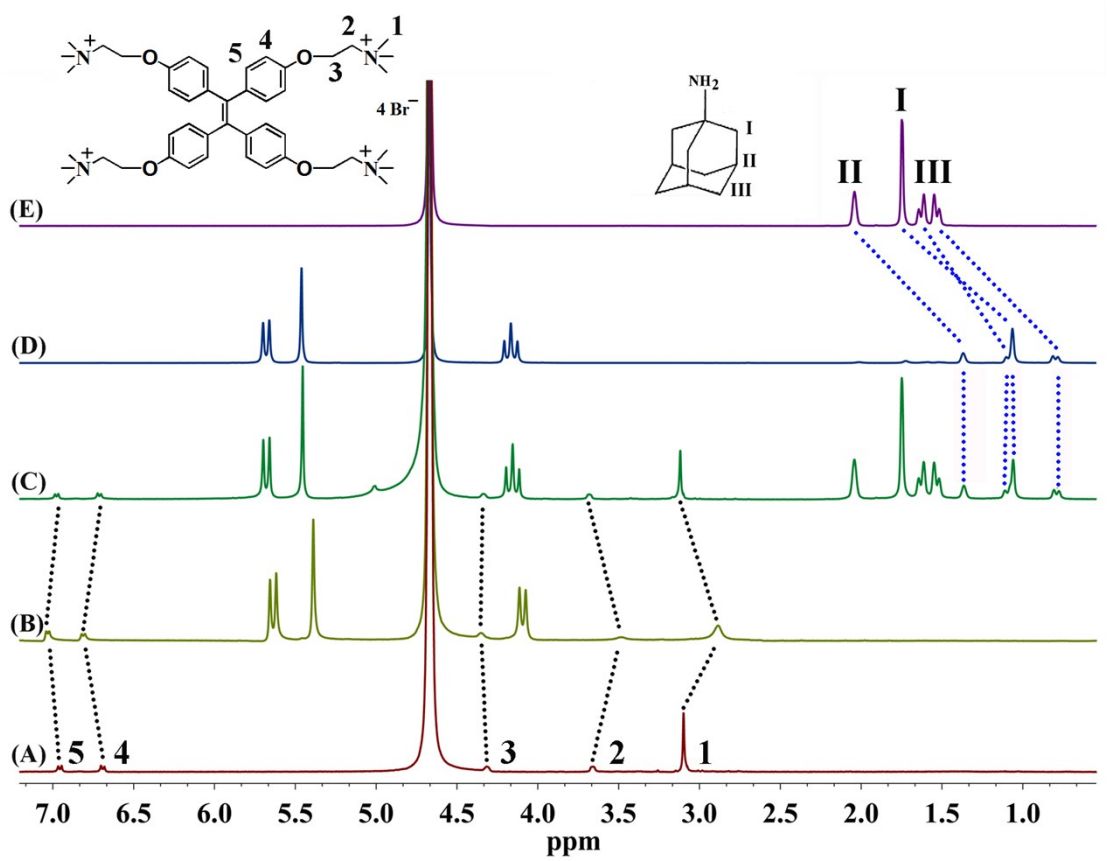

Figure S7. ^{1}H NMR spectra of TATPE (A), the complex Q[7]-TATPE (B), adding 15.0 equiv. Ada to B (C), the complex Q[7]-Ada (D), and Ada (E) recorded in D_2O at 25°C.

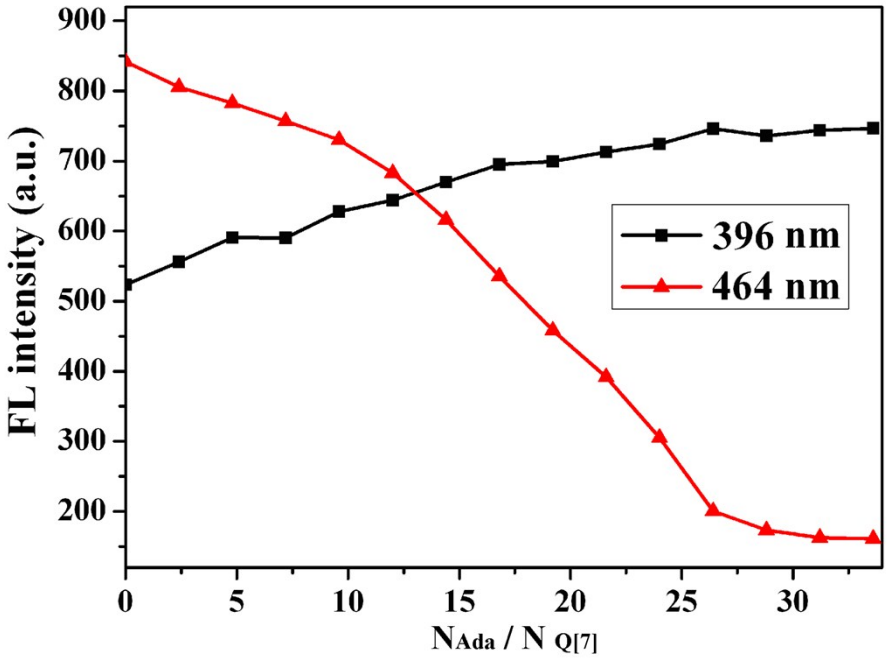

Figure S8. Curves of fluorescence intensity *versus* the molar ratio of $N_{Ada}/N_{Q[7]}$ measured at 464 and 396 nm in water.

Table S1. Complex stability constant (K_a), enthalpy ($\Delta H°$), and entropy changes ($T\Delta S°$) for Q[7]-TATPE.

Complex	K_a (M^{-4})	$\Delta H°$ (kJ mol^{-1})	$T\Delta S°$ (kJ mol^{-1})
Q[7]-TATPE	$(3.06 \pm 0.16) \times 10^5$	-93.62	-61.24